Degradation properties of organic light emitting diodes with modified interface charge density via dipolar doping studied by displacement current measurement

Mihiro Takeda, Alexander Hofmann, Wolfgang Brütting, Yutaka Noguchi

Angaben zur Veröffentlichung / Publication details:

Takeda, Mihiro, Alexander Hofmann, Wolfgang Brütting, and Yutaka Noguchi. 2025. "Degradation properties of organic light-emitting diodes with modified interface charge density via dipolar doping studied by displacement current measurement." *Advanced Electronic Materials* 11 (8): 2400788. https://doi.org/10.1002/aelm.202400788.

ADVANCED ELECTRONIC MATERIALS Open Access
www.advelectronicmat.de

Degradation Properties of Organic Light-Emitting Diodes with Modified Interface Charge Density via Dipolar Doping Studied by Displacement Current Measurement

*Mihiro Takeda, Alexander Hofmann, Wolfgang Brütting, and Yutaka Noguchi**

Accumulated charges at the interfaces of organic light-emitting diodes (OLEDs) often induce exciton quenching and lead to device degradation. This work delves into the correlations of the interface charge accumulation and degradation properties of tris(8-quinolinolato)aluminum (Alq_3)-based OLEDs. The interface accumulated charge density is modified by spontaneous orientation polarization (SOP) induced in the hole transport layer (HTL) by means of dipolar doping, where N,N′-bis(1-naphthyl)-N,N′-diphenyl-1,1′-biphenyl-4,4′-diamine (NPB) or tris(4-carbazoyl-9-ylphenyl) amine (TCTA) is employed as a hole transport material and 2,2′,2″-(1,3,5-Benzinetriyl)-tris-(1-phenyl-1-H-bensimidazole) (TPBi) as a dipolar dopant. It is confirmed that NPB cation acts as an exciton quencher, but TCTA cation does not, depending on the spectral overlap of Alq_3 emission and the absorption of the respective cations. On the other hand, the TCTA devices degrade much faster than the NPB devices. Moreover, the device lifetime is similar or even shorter for the doped devices despite less interface charge density. These results suggest that holes accumulated at the interface between the hole transport material and Alq_3 due to SOP are not mainly involved in the degradation mechanism. Furthermore, it is found that the charge traps generated due to degradation do not act as exciton quenchers, suggesting that they rather act as nonradiative recombination centers.

1. Introduction

Degradation of device performance is one of the main issues to be solved in the application of organic light-emitting diodes (OLEDs).[1–4] Previous work has suggested degradation mechanisms involving charge accumulation at the interfaces in the vicinity of the emission zone.[4–13] Kondakov et al. reported that the relatively weak carbon-nitrogen and carbon-carbon bonds in arylamine molecules are dissociated during device operation via the respective singlet excited states.[6,8] Such dissociation reactions are facilitated at an interface exhibiting charge accumulation, and likely mediated by the cationic molecular species, e.g., via exciton-polaron quenching (EPQ). The subsequent chemical products act as charge traps, exciton quenchers, and nonradiative recombination centers, leading to electroluminescent (EL) efficiency loss. Although their work focused on the archetypal fluorescent OLEDs, similar mechanisms have been reported in different types of OLEDs with phosphorescent and thermally activated delayed fluorescence emitters.[10,11]

The exciton distribution in the emission layer (EML) also plays a significant role in the device degradation as a narrow emission zone implies high carrier and exciton densities, which leads to faster degradation.[14,15] As a factor dominating the emission zone, the electron and hole mobilities of the transport layers have been suggested.[16] In addition, charge accumulation (or blocking) at the interface is also responsible for the exciton distribution.[17,18] The interface charge accumulation is thus considered as key to understand and suppress device degradation.

Spontaneous orientation polarization (SOP) is one of the dominant factors for charge accumulation at an interface between polar and nonpolar materials.[19–21] SOP has been frequently found in evaporated films of common OLED materials, particularly electron transport layer (ETL) and emission layer (EML) materials.[20–23] This macroscopic polarization phenomenon originates from the partial alignment of permanent dipole moments of molecules in the bulk of an evaporated film.[20,21,24] The spontaneous molecular orientation is inherited from the asymmetric situation at the film surface during the film deposition process, causing SOP in the out-of-plane direction.[25] The polarization charge of SOP appears at the hetero interfaces in stacked multiple layer OLEDs, leading to substantial

M. Takeda, Y. Noguchi
School of Science & Technology
Meiji University
Kawasaki 214–8571, Japan
E-mail: noguchi@meiji.ac.jp
A. Hofmann, W. Brütting
Institute of Physics
University of Augsburg
86135 Augsburg, Germany

The ORCID identification number(s) for the author(s) of this article can be found under https://doi.org/10.1002/aelm.202400788

DOI: 10.1002/aelm.202400788

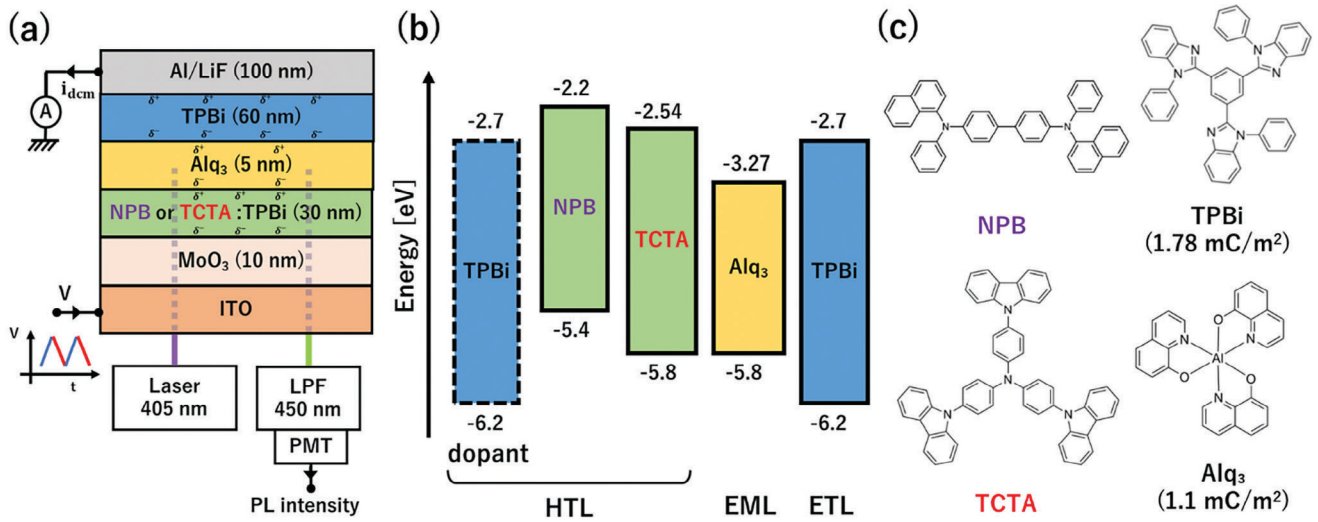

Figure 1. a) Schematic illustration of the device structure and the experimental setup of DCM-PL. b) Energy diagram of the materials. c) Chemical structure of the molecules. The SOP intensity of the neat film is indicated in the parenthesis.[20,28]

charge accumulation (typically ≈1 mC m^{-2}).[19,20] Importantly, the charge accumulation due to SOP occurs below the turn-on voltage of the OLED and results in the loss of external quantum efficiency (EQE) through exciton-polaron quenching (EPQ).[26,27] Moreover, it potentially impacts on the degradation properties of OLEDs.[4,13,20] Controlling SOP and optimizing its configurations in the device stack is thus important for improving device performance of OLEDs.[27,28]

Several methods have been reported to control SOP by adjusting substrate temperature or evaporation rate,[13,26,29–31] mixing of polar and nonpolar materials (dipolar doping),[32–36] and modifying molecular structure.[37–41] Using some of these methods, active control of SOP and its influence on OLED performance have recently been studied. Holmes et al. demonstrated an improvement in EQE by approximately 20% through the elimination of SOP in the ETL.[26,27] Afolayan et al. showed that eliminating SOP from the ETL of blue fluorescent OLEDs reduces operating voltage, increases EQE by 30%, and leads to a three-fold increase in device lifetime.[4] While these previous studies focused on the elimination of SOP in the device, we have proposed an alternative strategy to control interfacial charge accumulation properties, i.e., dipolar doping in the hole transport layer (HTL).[36] Although hole transport materials are typically nonpolar, dipolar doping induces SOP in the HTL. In the HTL/EML stacking structure, the positive polarization charge at the top of the HTL can partially compensate for the negative polarization charge at the bottom of the EML. Consequently, the net polarization charge at the HTL/EML interface is reduced to the difference between the SOP of the HTL and EML, provided that the SOP directions of these layers are the same. Similarly, the net polarization charge at the EML/ETL interface is determined. Dipolar doping allows us to control both the density and polarity of the accumulated charge at an interface without eliminating SOP of EML and ETL, providing a useful approach for studying the role of SOP in OLEDs.

In this study, we focused on the correlations between charge accumulation and degradation properties of tris(8-quinolinolato)aluminum (Alq_3)-based OLEDs, where the interface accumulated charge densities were modified by dipolar doping in the HTL (**Figure 1**a). N,N′bis(1-naphthyl)-N,N′-diphenyl-1,1′-biphenyl-4,4′-diamine (NPB) or tris(4-carbazoyl-9-ylphenyl) amine (TCTA) were used as a hole transport material and 2,2′,2″-(1,3,5-Benzinetriyl)-tris(1-phenyl-1-H-bensimidazole) (TPBi) as a dipolar dopant (Figure 1b,c). TPBi and Alq_3 exhibit significant SOP such as 1.78 mC m^{-2} and 1.1 mC m^{-2}, respectively, whereas NPB is almost nonpolar, and TCTA is nonpolar.[20,28] Consequently, negative polarization charge appears not only at the HTL/Alq_3 interface, but also at the Alq_3/TPBi interface, due to the larger SOP of TPBi compared to Alq_3. TPBi was employed as a dipolar dopant in this study because the SOP characteristics of the NPB and TCTA layers doped with TPBi were previously examined and confirmed that the mixed films exhibit significant SOP depending on the mixing ratio.[35] Moreover, the TPBi does not act as a hole trap since the highest occupied molecular orbital (HOMO) level of TPBi is sufficiently deeper than those of NPB and TCTA (Figure 1b), ensuring compatibility as a dipolar dopant.

The correlative behavior of charge accumulation and exciton quenching was examined by the simultaneous measurement of displacement current and photoluminescence (PL) intensity (DCM-PL technique, Figure 1a).[42] Therein a triangular wave voltage is applied to the device under ultraviolet (UV) light illumination. The detailed experimental conditions are described in the experimental section. DCM is a type of capacitance-voltage measurement that has been employed to assess charge injection and accumulation behaviors in organic semiconductor devices.[43] Since DCM detects current during both the forward and backward sweeps of the triangular wave voltage, it can distinguish between charge injection and extraction processes. Notably, DCM provides insights into charge trapping from the differences in current characteristics during the forward, backward, and consecutive voltage sweeps. In previous studies, a lock-in detection technique has been used to selectively detect PL signals from OLEDs, allowing the study of exciton quenching behaviors.[26,27,36] However, when measurements are limited

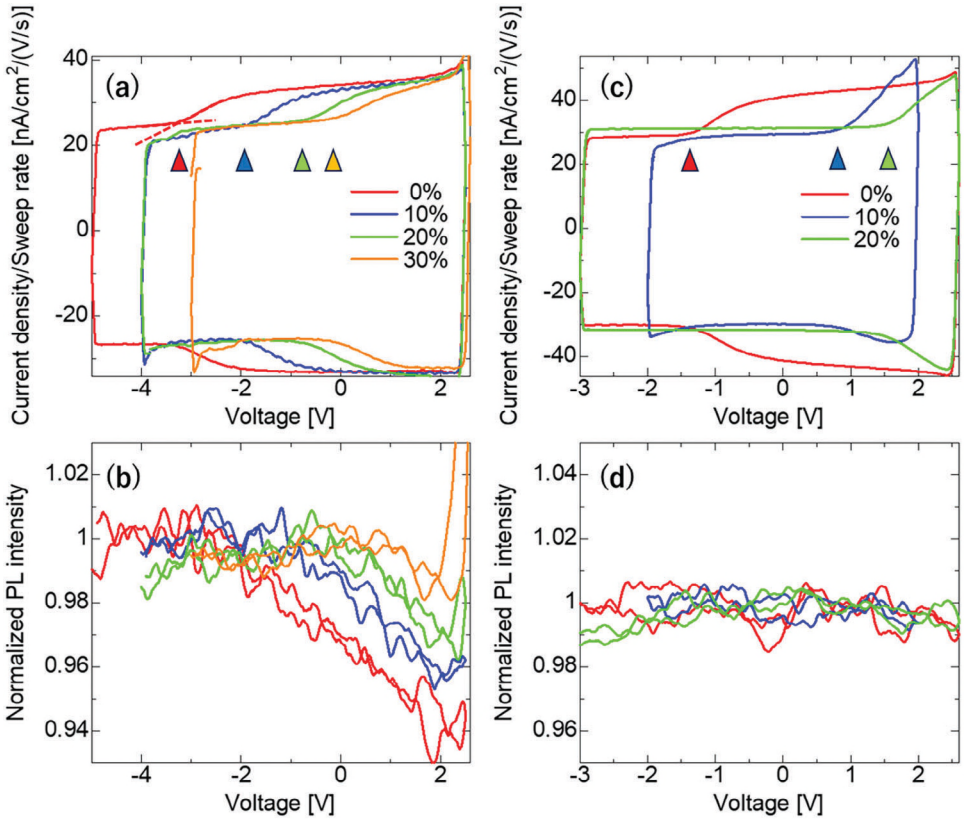

Figure 2. a,b) DCM-PL characteristics of the NPB device and c,d) the TCTA device with different TPBi doping ratio at a sweep rate of 10 and 100 V s^{-1}, respectively. a,c) DCM curves. b,d) Normalized PL intensity. The PL intensity curves were averaged over 25 cycles to improve the signal-to-noise ratio. The triangles in the DCM curves indicate the onset voltage of hole injection estimated from the intersection of the extrapolations of the displacement current before and after the transition as indicated by the broken lines in (a).

to below the turn-on voltage of OLEDs, lock-in detection becomes redundant. This situation enables simultaneous measurement of DCM and PL intensity characteristics, facilitating detailed analysis of the correlation between charge carrier behaviors and exciton dynamics. Further details have been reported elsewhere.[42]

Herein, we demonstrated a DCM-PL study on the device degradation of Alq_3-based OLEDs by controlling interface charge accumulation via dipolar doping of the HTL. The DCM-PL characteristics revealed that NPB cations act as an exciton quencher, but TCTA cations do not, depending on the spectral overlap of the Alq_3 emission and the absorption of the respective cations. On the other hand, the TCTA devices degraded much faster than the NPB devices. Moreover, the device lifetime was similar or even shorter for the dipolar doped devices despite less interface charge density. These results suggest that the accumulated holes induced at the interface between the HTL and Alq_3 due to SOP are not mainly involved in the degradation mechanism. Furthermore, we found that the charge traps generated due to degradation do not act as exciton quenchers, suggesting that they rather act as nonradiative recombination centers. Although interface charge accumulation and EPQ are often cited as causes of device degradation, our results suggest that the degradation of our devices occurs via a different mechanism. The combination of dipolar doping and DCM-PL is a powerful method for investigating the degradation mechanism of OLEDs, and whether or not EPQ is involved.

2. Results

2.1. Charge Accumulation and Exciton-Polaron Quenching in the Pristine Devices

Figure 2a,b show the DCM and normalized PL intensity curves (DCM-PL characteristics) of the NPB devices with different doping ratios of TPBi, respectively. Note that the DCM-PL characteristics were measured at voltages below the turn-on voltage of the device (≈2.5 V) to focus on the hole accumulation due to SOP. The PL intensity is normalized by the averaged PL intensity at the voltages just below the onset of hole injection (V_{inj}) in the "depletion state" to evaluate the EPQ characteristics induced by hole accumulation. In this study, V_{inj} is determined as the voltage at the intersection of the extrapolated displacement current in the depletion state and the slope of the transient to the "accumulation state", as indicated in the DCM curve of the undoped (0%) NPB device (Figure 2a). V_{inj} is observed at −3.2 V for the undoped device due to SOP of the Alq_3 and TPBi layers[20] and shifts to higher voltages with increasing doping ratio (Figure 2a) because SOP induced in the HTL partially compensates the negative polarization charge originating from the adjacent Alq_3 layer.[36] Increase of

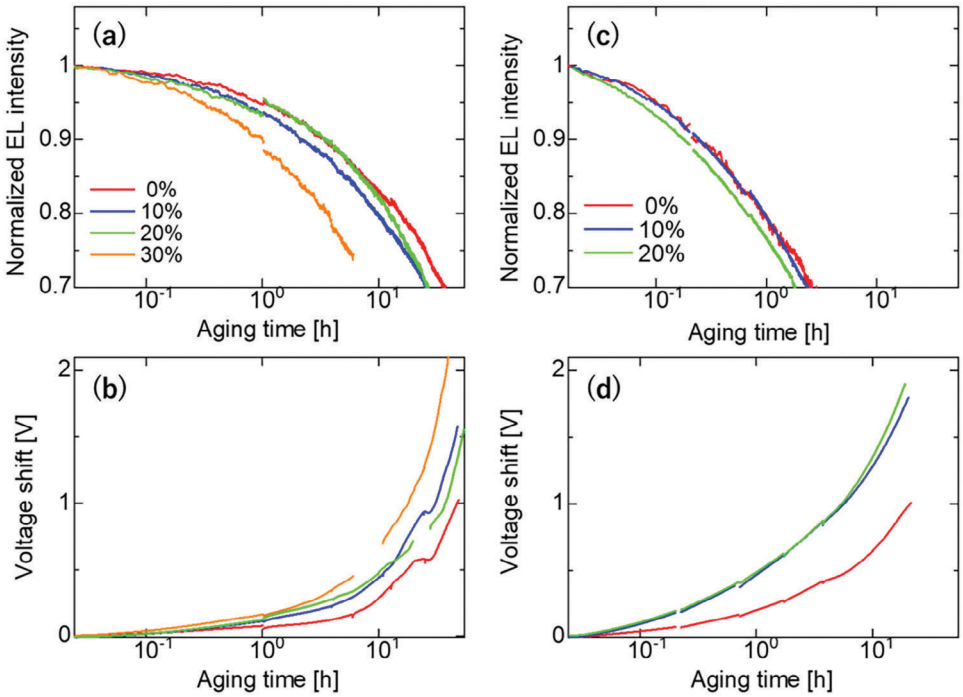

Figure 3. a,b) Evolutions of normalized EL intensity and voltage shift of the NPB device, and c,d) the TCTA device with different TPBi doping ratios at 50 mA cm^{-2}.

displacement current density above V_{inj} indicates hole accumulation at the HTL/Alq_3 interface, and simultaneously, reduction of the normalized PL intensity is observed at voltages higher than V_{inj} (Figure 2b). This reduction of PL intensity is well correlated to the hole accumulation behaviors and thus attributed to EPQ at the HTL/Alq_3 interface.

Figure 2c,d present the DCM-PL characteristics of the TCTA devices. Similar to the case of the NPB devices, the DCM curves (Figure 2c) reveal that dipolar doping efficiently reduces the accumulated holes at the HTL/Alq_3 interface; however, the normalized PL intensities do not change (Figure 2d), indicating that EPQ is negligibly small regardless of doping ratio (discussed later).

In the voltage range below the turn-on voltage, only photogenerated excitons are present in the Alq_3 layer. If exciton dissociation at the HTL/Alq_3 interface were relevant for the reduced PL intensity, it would be expected to be visible under reverse bias voltages (below V_{inj}), too. However, no such reduction is observed in Figure 2b,d, indicating that exciton dissociation is not efficient at these interfaces. Moreover, such a charge transfer (CT) state (or exciplex) is hardly formed at the NPB/Alq_3 interface[44] probably due to the bulky shape of Alq_3. We therefore presume that the contribution of CT state dissociation at the HTL/Alq_3 interface to PL quenching is negligible.[45]

The current density-voltage-luminance and current efficiency-current density characteristics of the pristine devices are shown in Figure S1 (Supporting Information). The current efficiency of the TCTA devices is typically higher than that of the NPB devices. Interestingly, although the current density is not significantly influenced, the luminance—and consequently, the current efficiency—of the NPB devices is improved by dipolar doping in the HTL. Notably, the luminous efficiency of the NPB devices with a doping ratio of 30% is enhanced by approximately 40% compared to the undoped device and is comparable to that of the TCTA devices. This enhancement in efficiency is consistent with the reduction of EPQ in the NPB devices due to dipolar doping.[17,26,27] Conversely, although the TCTA devices do not exhibit EPQ, an improvement in current efficiency is observed only for the 10%-doped device. A modification of the carrier balance factor would be a possible origin. Since mixed films of NPB:TPBi and TCTA:TPBi can exhibit exciplex emissions overlapping with the absorption band of Alq_3[46,47] they could act as an exciplex co-host[48,49] adjacent to the Alq_3 layer enhancing luminous efficiency. However, the EL spectrum of the NPB and TCTA devices indicates only Alq_3 emission (Figure S2, Supporting Information), and there is no clear evidence for the contribution of exciplex states. Further investigations are required to clarify the origin of this improvement.

2.2. Degradation Characteristics

Figure 3a,b display the evolutions of the normalized EL intensity and voltage shift of the NPB devices under a constant current operation at 50 mA cm^{-2}, respectively. In the undoped devices, the EL intensity decreases to 70% of the initial intensity after 34 h operation (LT70), while in the 10%- and 20%-doped devices, LT70 decreases to 24 h. In the 30%-doped device, the degradation of the EL intensity is more pronounced, i.e., LT70 is 8 h. On the other hand, LT70 of the TCTA devices is only about 2 h (Figure 3c), and is thus much shorter than that of the NPB devices. The shorter lifetime for the TCTA devices is consistent with the "unstable Alq_3 cationic model".[50,51] Since the energy barrier

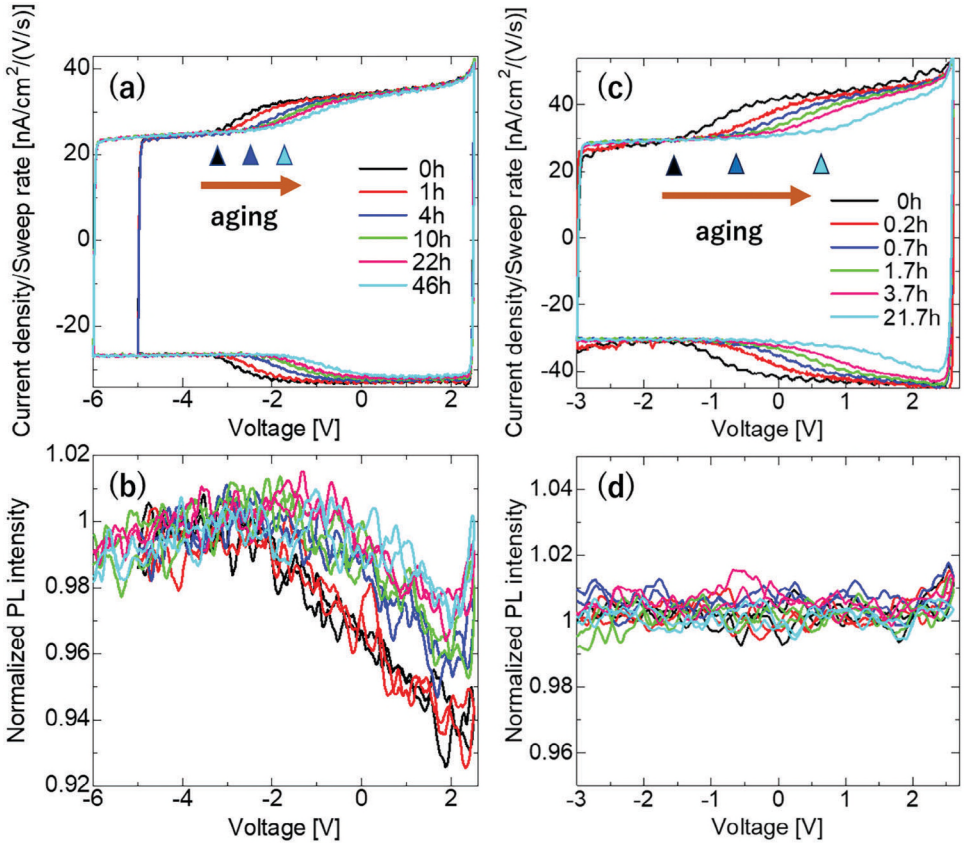

Figure 4. The DCM-PL characteristics of a,b) the undoped NPB device, and c,d) the undoped TCTA device at given operation time. The triangles in the DCM curves indicate the onset voltage of hole injection. The PL intensity curves were averaged over 25 cycles to improve the signal-to-noise ratio.

for holes at the TCTA/Alq_3 interface is lower than the one at the NPB/Alq_3 interface (Figure 1b), more holes penetrate into the Alq_3 layer in the TCTA devices, leading to faster degradation. In any case, dipolar doping does not mitigate degradation, though it reduces the accumulated hole density at the HTL/Alq_3 interface (Figure 2a,c). In addition, a significant voltage shift is observed in all devices according to the EL intensity loss (Figure 3b,d), suggesting the degradation of electrical properties, such as the formation of charge traps.

Figure 4a,b illustrate the DCM-PL characteristics of the undoped NPB device at given operation time during electrical degradation. V_{inj} in the DCM curve shifts toward higher voltages with proceeding operation time (Figure 4a). The V_{inj} shift corresponds to the reduction of the net interface charge density due to formation of hole traps (discussed later).[9–11] Additionally, the normalized PL intensity curves also shift to higher voltages accordingly (Figure 4b). As a result, the EPQ at the HTL/Alq_3 interface in the sub-turn-on voltage region was even suppressed in the degraded devices. Interestingly, the slope of the PL reduction over the accumulated charge density did not change even after degradation (Figure S3, Supporting Information), suggesting that the EPQ rate constant is similar. Consequently, a contribution of EPQ to degradation was not detectable.

Figure 4c,d present the DCM-PL characteristics of the undoped TCTA device. Similar to the NPB devices, the V_{inj} shift during device degradation is observed, though it is much larger in the TCTA devices than in the NPB devices even with shorter operation duration. On the other hand, the normalized PL intensity does not depend on the applied voltage at any given operation time, indicating that the charge accumulation at the HTL/Alq_3 interface is not responsible for the efficiency loss even in the degraded devices. These trends are commonly observed in the doped devices (Figures S4 and S5, Supporting Information).

We examined the properties of charge traps formed in the degraded devices by the cycle dependence of the DCM-PL characteristics.[10,11] Prior to the application of a triangular wave voltage, a constant reverse bias of −6 and −3 V was applied to the NPB and TCTA device, respectively, for 10 s under intense UV light illumination at a wavelength of 400 nm. This procedure facilitates the release or annihilation of trapped charges from the device (**Figure** 5a). Consequently, the trap sites can be assumed to be empty or only partially occupied before the DCM-PL measurement (Figure 5b). By applying successive cycles of triangular wave voltages, the traps are occupied by the injected charges (Figure 5c) and the device transfers to the steady state (Figure 5d).

Figure 6a,b show the cycle dependence of the DCM-PL characteristics of the undoped NPB device after 46 h aging. Only the results of the first and fifth cycles are shown for clarity. The DCM curve of the pristine unaged device is also displayed as a reference. Note that the PL intensity is not normalized to examine its cycle dependence. The V_{inj} for the first cycle is –5.1 V, while it increases to −1.8 V for the fifth cycle, indicating that

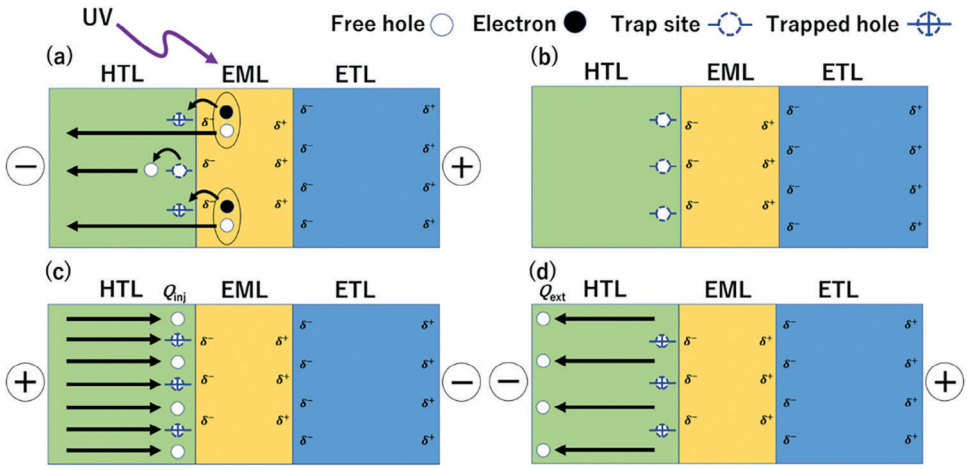

Figure 5. Schematic illustrations of trap occupation state at the HTL/EML interface during the DCM-PL measurement. The polarity of the applied voltage is indicated outside of the device. a) Release or annihilation of the trapped holes before the measurement due to absorption of UV light in the HTL or the adjacent EML. b) Unoccupied hole traps before charge injection of the 1st cycle of the voltage sweep. c) Trap filling process during charge injection with the amount of Q_{inj} in the 1st cycle of the voltage sweep. d) Extraction of the accumulated free holes, where the amount is less than the injected holes ($Q_{ext} < Q_{inj}$), while the trapped holes remain in the device for the consecutive voltage sweeps.

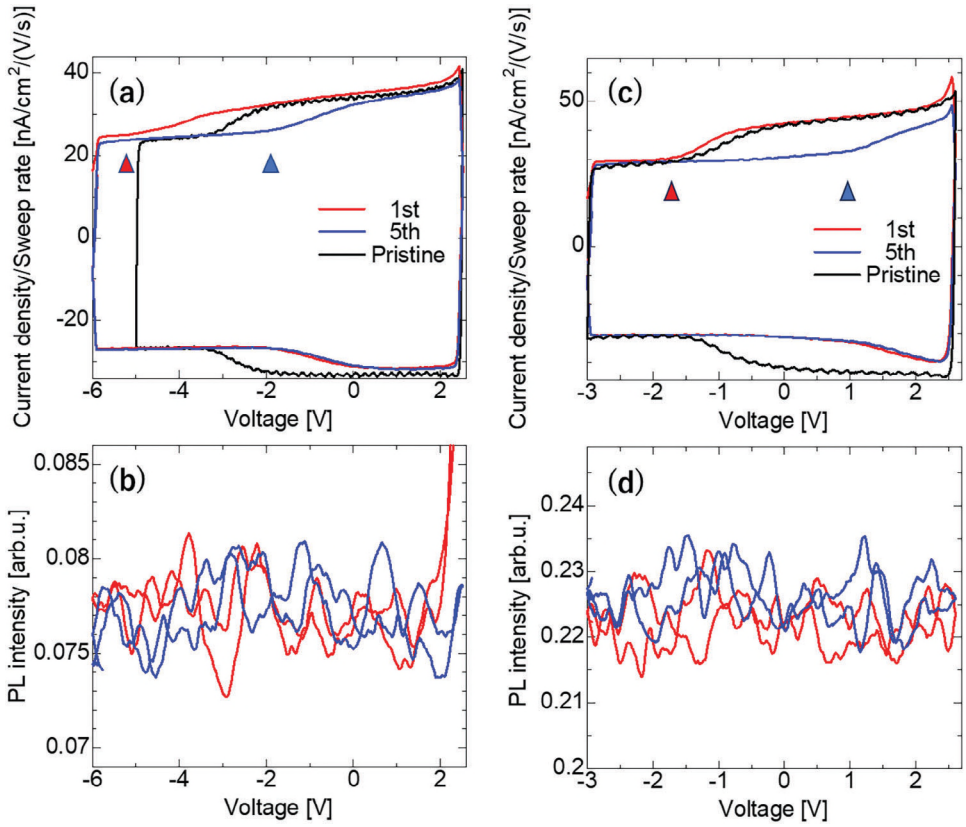

Figure 6. a,b) Cycle dependence of the DCM-PL characteristics of the undoped NPB device, and c,d) the undoped TCTA device after aging. Triangles indicate the injection voltage. The PL intensity curves were not averaged and normalized. The DCM curves of the pristine devices are also shown as a reference.

significant amount of injected holes (≈1.04 mC m^{-2}) are trapped in the device. Since this voltage shift was not observed in the pristine device (see Figure S6, Supporting Information), the charge traps are formed due to device operation. In the pristine device, the V_{inj} is observed at −3.2 V, which is 1.4 V lower than that in the 5th cycle of the degraded device (Figure 6a), suggesting that the negative interface charge due to SOP of Alq_3 is partially compensated by the trapped holes. Conversely, the V_{inj} in the pristine state is 1.9 V higher than that in the first cycle after degradation, indicating the presence of trapped electrons before the measurement. The trapped electrons are eliminated by the injected holes during the first cycle of the DCM-PL measurement, and the trapped holes remain in the device (Figure 5d). Despite such differences of trap site occupation, the PL intensity (not normalized) characteristics of the first and subsequent cycles are almost identical (Figure 6b), indicating that the trap sites and the trapped charges do not contribute to PL quenching.

Figure 6c,d present the DCM-PL characteristics of the undoped TCTA devices after 21.7 h aging. Similar to the NPB devices, a notable shift of the V_{inj} is observed, i.e., −1.8 V in the first cycle, while it is +1.0 V in the fifth cycle. In the pristine state, the hole injection voltage appears at −1.5 V (Figure 4c). The negative shift of the injection voltage is −0.3 V for the undoped TCTA device. This result suggests that the trap sites generated in the TCTA device are likely to trap holes. Additionally, no cycle dependence is seen in the PL intensity characteristics (Figure 6d), suggesting that the trap sites and the trapped charges do not contribute to PL quenching here as well.

3. Discussion

3.1. Correlations of Charge Accumulation and Degradation Properties

Dipolar doping in the HTL controls the charge accumulation properties at the HTL/EML interface, and it is thus a useful technique to investigate the correlations between charge accumulation and device degradation. Moreover, the DCM-PL characteristics revealed that EPQ is significant in the NPB devices, while it is negligible in the TCTA devices. These observations agree well with the absorption band of the respective polarons, i.e., the absorption band of NPB cations overlaps with the emission spectrum of Alq_3, while that of TCTA cations does not (see Figure S1, Supporting Information of ref. [52]). Although the EPQ was suppressed by dipolar doping (Figure 2b) or by using a transparent material (TCTA) for the Alq_3 emission (Figure 2d), the device lifetime was unaffected or even reduced (Figure 3a,c). These results indicate that the hole accumulation induced by SOP at the HTL/Alq_3 interface is unlikely to contribute to the degradation mode of our devices, though molecular decomposition via the excited state of cation species is often referred as a trigger of degradation.[3,12,53]

The conductivity of electron and hole transport layers has also been suggested as a significant factor in device degradation. Qin et al. proposed a degradation model based on carrier lifetimes within the device.[16] According to this model, higher charge carrier mobilities in the transport layers result in longer carrier lifetimes within the exciton formation zone at a constant current density, leading to a broader emission zone and extended device lifetime. Since dipolar doping often deteriorates HTL conductance, likely due to the dipolar disorder effect,[34,36] we examined the conductance of the doped films by impedance spectroscopy measurements at a sub-turn-on voltage of 2 V (Figure S7, Supporting Information). In this voltage range, only hole injection occurs in the device, allowing the selective detection of the individual conductance of the HTL.[36] The results revealed that the conductance of TCTA:TPBi films decreases markedly with increasing doping ratios, while the conductance of NPB:TPBi films remains comparable to that of undoped NPB films. The degradation characteristics of the doped devices deviate from the trends predicted by the carrier lifetime model. Specifically, the degradation of TCTA devices is relatively unaffected by the TPBi doping ratio, whereas that of NPB devices decreases significantly with doping. Furthermore, considering the HOMO offsets at the interfaces, a higher hole-blocking ability is expected at the NPB/Alq_3 interface compared to the TCTA/Alq_3 interface. Consequently, the emission zone in the NPB devices is confined to the NPB/Alq_3 interface, while in the TCTA devices, the emission zone extends into the Alq_3 layer. This scenario is supported by device simulations (Figure S8, Supporting Information). Although a broader emission zone generally correlates with longer device lifetimes, our experimental results indicate the opposite trend, with the TCTA devices exhibiting much shorter lifetimes than the NPB devices. We thus speculate that the degradation of Alq_3 through the unstable cationic state is dominant in our devices.[50,51] Another possible contributing factor is parasitic leakage current through the device. Relatively large leakage currents were observed in the TCTA devices at the low voltage region after degradation (not shown), compared to those in the NPB devices, although the exact origin remains unclear. While this leakage current was not severe enough to cause catastrophic failure, it could alter the relative conductance of HTL and ETL, thereby potentially facilitating device degradation.

Kondakov et al. found a negative linear relation between the luminous efficiency and V_{inj} in the degradation process, where the shift of V_{inj} corresponds to the amount of trapped holes.[5] This negative linear relation has frequently been observed in various types of OLEDs,[10,11] and thus suggests the presence of a common origin leading to the loss of luminous efficiency, such as charge traps acting as a nonradiative recombination center and an exciton quencher. To evaluate the contribution of trapped holes to luminance loss, we constructed **Figure 7**, which plots the normalized EL intensity as a function of V_{inj} of the NPB and TCTA devices during the degradation process. The normalized EL intensity and V_{inj} at given operation time were derived from Figures 3 and 4 (or Figure S4, Supporting Information), respectively. Note that the results of the 10%- and 20%-doped TCTA devices during degradation are not shown in Figure 7 because of the leakage current in the DCM curves at the low voltage region. A negative linear trend is seen in the undoped and 10%-doped devices. Surprisingly, a similar slope is observed for the undoped NPB and TCTA devices, suggesting that the charge traps formed in these devices similarly contribute to the efficiency loss. On the other hand, nonlinearity appears for the 20%- and 30%-doped devices. A possible explanation of the nonlinearity is the shift in the location of the hole traps as the negative interface charge at the HTL/Alq_3 interface becomes compensated. For instance, as this compensation occurs, the charge accumulation zone may

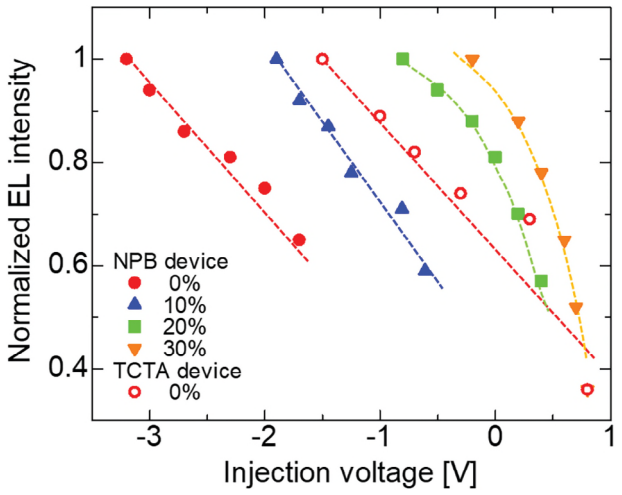

Figure 7. Normalized EL intensity as a function of injection voltage during device degradation. Broken lines are a guide for the eye.

shift toward the Alq_3/TPBi interface due to the negative interface charge at this boundary. Such a transition is likely to occur in devices with higher doping ratio.

The DCM-PL characteristics revealed that the device lifetime does not depend on the amount of accumulated charge induced by SOP and subsequent EPQ. Furthermore, the cycle dependence of the DCM-PL characteristics indicated that the trap sites do not contribute to exciton quenching. Accordingly, they are probably responsible for the efficiency loss by acting as a nonradiative recombination center, though the chemical origin of the trap sites has not been identified. This hypothesis is consistent with the observation of the linear relation with a similar slope in the different HTL devices, since the efficiency loss linearly depends on the density of the nonradiative recombination centers.[10]

4. Conclusion

Correlations between the charge accumulation and degradation properties of Alq_3-based OLEDs incorporating dipolar doped HTLs were investigated by the DCM-PL technique. The accumulated charge density at the HTL/Alq_3 interface was modified by using dipolar doping in HTLs. Regardless of the HTLs, however, the lifetime of the doped devices was similar or even shorter than that of the respective undoped device. On the other hand, the lifetime of the NPB devices was much longer than that of the TCTA devices, though they indicate significant EPQ due to energy transfer from Alq_3 excitons to NPB cations. Moreover, the DCM-PL characteristics revealed that the charge traps generated during device aging do not act as an exciton quencher. The amount of the trapped charge was approximately proportional to the efficiency loss, and surprisingly, the slopes of the linear relation observed in the NPB and TCTA devices are similar to each other. Our results clearly indicate that the accumulated charges due to SOP and subsequent EPQ do not cause the efficiency loss during device degradation. It is rather the generated charge traps that are directly involved, probably by acting as a nonradiative recombination centers. DCM-PL in combination with dipolar doping is a promising technique for elucidating the degradation mechanisms of OLEDs.

5. Experimental Section

Materials: TPBi and Alq_3 exhibit significant SOP such as 1.78 and 1.1 mC m^{-2}, respectively, while NPB's SOP is small (0.16 mC m^{-2}), and TCTA is nonpolar.[20,28] Significant SOP of the NPB:TPBi and TCTA:TPBi mixed films was confirmed previously.[35] Moreover, TPBi is unlikely to act as a hole trap in NPB and TCTA, since its HOMO level is deeper than that of NPB and TCTA. The study thus employed TPBi as a dipolar dopant. The doping concentration to cancel out the interface charges from TPBi and Alq_3 was set at 0–30% for NPB devices and 0–20% for TCTA devices. All organic materials used in this study were sublimed grade (>99.5%) purchased from Luminescence Technology Corp., and used without further purification.

Device Fabrication: An indium-tin-oxide (ITO)-coated glass substrate was purchased from Q-Lights Co. Ltd. The ITO thickness is 50 nm and the sheet resistance is 50 Ω/sq. The ITO-coated glass substrate was cleaned by sequential ultrasonication in detergent, pure water, acetone, and isopropanol. Then the substrate was annealed at 150 °C for 1.5 hours (in a N_2-filled glove box). Subsequently, a plasma treatment was performed, just before the substrate was loaded to the vacuum chamber for material deposition. All organic materials were successively deposited using a conventional thermal evaporation technique at a deposition rate of ≈1.0 Å s^{-1} without controlling substrate temperature followed by LiF and Al deposition. A base pressure during the film deposition was ≈10^{-4} Pa. The device was then transferred to a N_2-filled glove box for encapsulation. Note that the device was exposed to air for a short time during transportation. The dimensions of the device active area were 0.2 × 0.2 cm^2.

Device Characterization: For the DCM-PL, the study used a function generator (3390, Keithley) as the voltage source, with the sweep rate of the triangular-wave voltage ranging from 10 to 1000 V s^{-1}. The current was detected using a current amplifier (SR570, Stanford Research Systems). A UV laser was used at a wavelength of 405 nm (M00846504, THORLABS) as the excitation light source. The excitation light was nonpolarized, and the incident and detection angles were 0° with reference to the surface normal direction. The study measured the PL intensity through an LPF (cut-in wavelength: 450 nm) using a photomultiplier-tube module (H11901-20, Hamamatsu Photonics) with another current amplifier (SR570, Stanford Research Systems). The voltage, current, and PL intensity were recorded through an analog-to-digital (A/D) converter (USB-6210, National Instruments).[42] Post-electrical degradation detrapping was carried out by illuminating an intense UV light at a wavelength of 400 nm from a Xe lamp (MAX-302, Asahi spectra Co., Ltd.) through a band pass filter with applying reverse bias voltage. Degradation was induced by applying a constant current density (50 mA cm^{-2}), and the evolutions of voltage and EL intensity were recorded. A two channel source measure unit (2612A, Keithley) was used for the measurement. The DCM-PL characteristics at a given operation time were measured separately.

Supporting Information

Supporting Information is available from the Wiley Online Library or from the author.

Acknowledgements

This work was supported by the JSPS Bilateral Program Number JPJSBP120233508 and the DAAD project no. 57663382.

Conflict of Interest

The authors declare no conflict of interest.

Data Availability Statement

The data that support the findings of this study are available from the corresponding author upon reasonable request.

Keywords

degradation, dipolar doping, interface charge, organic light-emitting diode, spontaneous orientation polarization

Received: October 12, 2024
Revised: January 5, 2025
Published online: January 15, 2025

[1] S. Scholz, D. Kondakov, B. Lüssem, K. Leo, *Chem. Rev.* **2015**, *115*, 8449.
[2] H. Zhao, C. E. Arneson, D. Fan, S. R. Forrest, *Nature* **2024**, *626*, 300.
[3] B. Van Der Zee, Y. Li, G. J. A. H. Wetzelaer, P. W. M. Blom, *Phys. Rev. Appl.* **2022**, *18*, 064002.
[4] E. O. Afolayan, I. Dursun, C. Lang, E. Pakhomenko, M. Kondakova, M. Boroson, M. Hickner, R. J. Holmes, N. C. Giebink, *Phys. Rev. Appl.* **2022**, *17*, L051002.
[5] D. Y. Kondakov, J. R. Sandifer, C. W. Tang, R. H. Young, *J. Appl. Phys.* **2003**, *93*, 1108.
[6] D. Y. Kondakov, *J. Appl. Phys.* **2008**, *104*, 084520.
[7] V. V. Jarikov, D. Y. Kondakov, *J. Appl. Phys.* **2009**, *105*, 034905.
[8] D. Y. Kondakov, C. T. Brown, T. D. Pawlik, V. V. Jarikov, *J. Appl. Phys.* **2010**, *107*, 024507.
[9] Y. Noguchi, T. Tamura, H. Kim, H. Ishii, *J. Photonics Energy* **2012**, *2*, 021214.
[10] T. D. Schmidt, L. Jäger, Y. Noguchi, H. Ishii, W. Brütting, *J. Appl. Phys.* **2015**, *117*, 215502.
[11] Y. Noguchi, H. Kim, R. Ishino, K. Goushi, C. Adachi, Y. Nakayama, H. Ishii, *Org. Electron.* **2015**, *17*, 184.
[12] Y. Zhang, H. Aziz, *ACS Appl. Mater. Interfaces* **2016**, *8*, 14088.
[13] Y. Esaki, M. Tanaka, T. Matsushima, C. Adachi, *Adv. Electron. Mater.* **2021**, *7*, 2100486.
[14] Y. Zhang, J. Lee, S. R. Forrest, *Nat. Commun.* **2014**, *5*, 5008.
[15] H. Zhao, W. Liu, R. Cui, S. Feng, Y. Sun, L. Zhou, D. Qin, *Displays* **2022**, *74*, 102287.
[16] D. Qin, J. Li, *Phys. Status Solidi* **2024**, 2400566.
[17] B. Ruhstaller, S. A. Carter, S. Barth, H. Riel, W. Riess, J. C. Scott, *J. Appl. Phys.* **2001**, *89*, 4575.
[18] R. Coehoorn, X. Lin, C. H. L. Weijtens, S. Gottardi, H. van Eersel, *Phys. Rev. Appl.* **2021**, *16*, 034048.
[19] Y. Noguchi, Y. Miyazaki, Y. Tanaka, N. Sato, Y. Nakayama, T. D. Schmidt, W. Brütting, H. Ishii, *J. Appl. Phys.* **2012**, *111*, 114508.
[20] Y. Noguchi, W. Brütting, H. Ishii, *Jpn. J. Appl. Phys.* **2019**, *58*, SF0801.
[21] A. Hofmann, M. Schmid, W. Brütting, *Adv. Opt. Mater.* **2021**, *9*, 2101004.
[22] K. Osada, K. Goushi, H. Kaji, C. Adachi, H. Ishii, Y. Noguchi, *Org. Electron.* **2018**, *58*, 313.
[23] B. A. Naqvi, M. Schmid, E. Crovini, P. Sahay, T. Naujoks, F. Rodella, Z. Zhang, P. Strohriegl, S. Bräse, E. Zysman-Colman, W. Brütting, *Front. Chem.* **2020**, *8*, 750.
[24] E. Ito, Y. Washizu, N. Hayashi, H. Ishii, N. Matsuie, K. Tsuboi, Y. Ouchi, Y. Harima, K. Yamashita, K. Seki, *J. Appl. Phys.* **2002**, *92*, 7306.
[25] K. Bagchi, N. E. Jackson, A. Gujral, C. Huang, M. F. Toney, L. Yu, J. J. De Pablo, M. D. Ediger, *J. Phys. Chem. Lett.* **2019**, *10*, 164.
[26] J. S. Bangsund, J. R. Van Sambeek, N. M. Concannon, R. J. Holmes, *Sci. Adv.* **2020**, *6*, eabb2659.
[27] E. Pakhomenko, S. He, R. J. Holmes, *Chem. Phys. Rev.* **2023**, *4*, 021308.
[28] Y. Noguchi, Y. Tanaka, H. Ishii, W. Brütting, *Synth. Met.* **2022**, *288*, 117101.
[29] S. He, E. Pakhomenko, R. J. Holmes, *ACS Appl. Mater. Interfaces* **2022**, *15*, 1652.
[30] A. Cakaj, M. Schmid, A. Hofmann, W. Brütting, *ACS Appl. Mater. Interfaces* **2023**, *15*, 54721.
[31] M. Ohara, H. Hamada, N. Matsuura, Y. Tanaka, H. Ishii, *ACS Appl. Mater. Interfaces* **2023**, *15*, 57427.
[32] L. Jäger, T. D. Schmidt, W. Brütting, *AIP Adv.* **2016**, *6*, 095220.
[33] T. Morgenstern, M. Schmid, A. Hofmann, M. Bierling, L. Jäger, W. Brütting, *ACS Appl. Mater. Interfaces* **2018**, *10*, 31541.
[34] A. J. L. Hofmann, S. Züfle, K. Shimizu, M. Schmid, V. Wessels, L. Jäger, S. Altazin, K. Ikegami, M. R. Khan, D. Neher, H. Ishii, B. Ruhstaller, W. Brütting, *Phys. Rev. Appl.* **2019**, *12*, 064052.
[35] Y. Noguchi, K. Osada, K. Ninomiya, H. D. C. N. Gunawardana, K. R. Koswattage, H. Ishii, *J. Soc. Inf. Disp.* **2021**, *29*, 29.
[36] Y. Noguchi, A. Hofmann, W. Brütting, *Adv. Opt. Mater.* **2022**, *10*, 2201278.
[37] T. Isoshima, Y. Okabayashi, E. Ito, M. Hara, W. W. Chin, J. W. Han, *Org. Electron. Phys., Mater. Appl.* **2013**, *14*, 1988.
[38] M. Tanaka, M. Auffray, H. Nakanotani, C. Adachi, *Nat. Mater.* **2022**, *21*, 819.
[39] W.-C. Wang, K. Nakano, D. Hashizume, C.-S. Hsu, K. Tajima, *ACS Appl. Mater. Interfaces* **2022**, *14*, 18773.
[40] W. C. Wang, K. Nakano, C. S. Hsu, K. Tajima, *ACS Appl. Mater. Interfaces* **2023**, *15*, 20294.
[41] M. Tanaka, *Nat. Commun.* **2024**, *15*, 9297.
[42] Y. Noguchi, K. Ninomiya, K. Sato, *J. Phys. Chem. C* **2022**, *126*, 18520.
[43] Y. Noguchi, Y. Tanaka, Y. Miyazaki, N. Sato, Y. Nakayama, H. Ishii, in *Physics of Organic Semiconductors: Second, Completely New Revised Edition* (Eds.: W. Brütting, C. Adachi), Wiley-VCH, Weinheim, Germany **2012**, Ch. 5.
[44] J. Song, C. Wang, Y. Guan, X. Bao, W. J. Li, L. Chen, L. Niu, *RSC Adv.* **2023**, *13*, 23619.
[45] S. Gottardi, M. Barbry, R. Coehoorn, H. Van Eersel, *Appl. Phys. Lett.* **2019**, *114*, 073301.
[46] W. Song, J. Y. Lee, *Appl. Phys. Lett.* **2015**, *106*, 123306.
[47] V. Jankus, C. J. Chiang, F. Dias, A. P. Monkman, *Adv. Mater.* **2013**, *25*, 1455.
[48] Y. S. Park, S. Lee, K. H. Kim, S. Y. Kim, J. H. Lee, J. J. Kim, *Adv. Funct. Mater.* **2013**, *23*, 4914.
[49] J. W. Park, K. H. Cho, Y. M. Rhee, *Int. J. Mol. Sci.* **2022**, *23*, 5940.
[50] H. Aziz, Z. D. Popovic, N.-X. Hu, A.-M. Hor, G. Xu, *Science* **1999**, *283*, 1900.
[51] Z. D. Popovic, H. Aziz, N. Hu, A. Ioannidis, P. N. M. Anjos, Z. D. Popovic, H. Aziz, N. Hu, *J. Appl. Phys.* **2009**, *89*, 4673.
[52] B. Nell, K. Ortstein, O. V. Boltalina, K. Vandewal, *J. Phys. Chem. C* **2018**, *122*, 11730.
[53] N. C. Giebink, B. W. D'Andrade, M. S. Weaver, P. B. MacKenzie, J. J. Brown, M. E. Thompson, S. R. Forrest, *J. Appl. Phys.* **2008**, *103*, 044509.